RAPID REPORT

Inositol-1,4,5-trisphosphate-dependent Ca^{2+} signalling in cat atrial excitation–contraction coupling and arrhythmias

Aleksey V. Zima and Lothar A. Blatter

Department of Physiology, Loyola University Chicago, Stritch School of Medicine, 2160 S. First Avenue, Maywood, IL 60153, USA

Inositol-1,4,5-trisphosphate (IP_3)-dependent Ca^{2+} release represents the major Ca^{2+} mobilizing pathway responsible for diverse functions in non-excitable cells. In the heart, however, its role is largely unknown or controversial. In intact cat atrial myocytes, endothelin (ET-1) increased basal $[Ca^{2+}]_i$ levels, enhanced action potential-evoked $[Ca^{2+}]_i$ transients, caused $[Ca^{2+}]_i$ transients with alternating amplitudes (Ca^{2+} alternans), and facilitated spontaneous Ca^{2+} release from the sarcoplasmic reticulum (SR) in the form of Ca^{2+} sparks and arrhythmogenic Ca^{2+} waves. These effects were prevented by the IP_3 receptor (IP_3R) blocker aminoethoxydiphenyl borate (2-APB), suggesting the involvement of IP_3-dependent SR Ca^{2+} release. In saponin-permeabilized myocytes IP_3 and the more potent IP_3R agonist adenophostin increased basal $[Ca^{2+}]_i$ and the frequency of spontaneous Ca^{2+} sparks. In the presence of tetracaine to eliminate Ca^{2+} release from ryanodine receptor (RyR) SR Ca^{2+} release channels, IP_3 and adenophostin triggered unique elementary, non-propagating IP_3R-dependent Ca^{2+} release events with amplitudes and kinetics that were distinctly different from classical RyR-dependent Ca^{2+} sparks. The effects of IP_3 and adenophostin were prevented by heparin and 2-APB. The data suggest that IP_3-dependent Ca^{2+} release increases $[Ca^{2+}]_i$ in the vicinity of RyRs and thus facilitates Ca^{2+}-induced Ca^{2+} release during excitation–contraction coupling. It is concluded that in the adult mammalian atrium IP_3-dependent Ca^{2+} release enhances atrial Ca^{2+} signalling and exerts a positive inotropic effect. In addition, by facilitating Ca^{2+} release, IP_3 may also be an important component in the development of Ca^{2+}-mediated atrial arrhythmias.

(Received 21 November 2003; accepted after revision 26 January 2004; first published online 30 January 2004)
Corresponding author L. A. Blatter: Department of Physiology, Loyola University Chicago, Stritch School of Medicine, 2160 S. First Ave., Maywood, IL 60153, USA. Email: lblatte@lumc.edu

During each heart beat an action potential depolarizes the cell membrane of cardiac myocytes to allow Ca^{2+} entry through voltage-gated Ca^{2+} channels. This relatively small amount of Ca^{2+} entry triggers a massive Ca^{2+}-induced Ca^{2+} release (CICR) from intracellular SR Ca^{2+} stores by activating Ca^{2+}-sensitive Ca^{2+} release channels (ryanodine receptors, RyRs) in the SR membrane. CICR represents the key step in excitation–contraction (E-C) coupling which provides the necessary amount of cytoplasmic Ca^{2+} to activate the contractile proteins resulting in contraction of the heart. Ca^{2+} release occurs from clusters of RyRs (Blatter *et al.* 1997) in the form of localized non-propagating elevations of $[Ca^{2+}]_i$, termed Ca^{2+} sparks. Here we use the term Ca^{2+} spark to refer strictly to elementary Ca^{2+} release events from RyRs. Ca^{2+} sparks are the building blocks of Ca^{2+} release and the spatio-temporal summation of these elementary Ca^{2+} release events forms the whole cell $[Ca^{2+}]_i$ transient during E-C coupling.

IP_3 is an important activator of a specific class of SR Ca^{2+} release channels, i.e. IP_3 receptors (IP_3Rs). IP_3-dependent Ca^{2+} release represents the main avenue of intracellular Ca^{2+} release in electrically non-excitable cells (Berridge, 1997). In contrast, in cardiac tissue the main pathway of Ca^{2+} release occurs through RyRs, and IP_3Rs are expressed at 1–2 orders of magnitude lower density than RyRs (Perez *et al.* 1997). Although IP_3-dependent Ca^{2+} release in cardiac tissue was demonstrated early on (Hirata *et al.* 1984; Fabiato, 1986; Nosek *et al.* 1986), the role of IP_3 in E-C coupling and cardiac function in the adult mammalian heart has remained highly controversial (Marks, 2000; Bers, 2001; Blatter *et al.* 2003).

 DOI: 10.1113/jphysiol.2003.058529

There is evidence that IP_3-dependent signalling may be important during development (Rosemblit *et al.* 1999; Poindexter *et al.* 2001) and cardiac injury (Mouton *et al.* 1992; Jacobsen *et al.* 1996; Woodcock *et al.* 1997, 1998; Harrison *et al.* 1998; Yamada *et al.* 2001), or may be relevant to the regulation of specific cellular functions such as propagation of electrical signals in Purkinje fibres, regulation of organellar and nuclear membrane permeability, Ca^{2+}-dependent gene transcription, cardiac hypertrophy signalling and cell growth (e.g. Jaconi *et al.* 2000; for references see Bers, 2001). Atrial tissue expresses functional IP_3-receptors at 6–10 times higher levels than ventricular myocytes and IP_3Rs seem to colocalize with RyRs in the subsarcolemmal space (Lipp *et al.* 2000; Mackenzie *et al.* 2002). Although it has been proposed that IP_3-dependent Ca^{2+} signalling plays a direct role in atrial E-C coupling under physiological as well as pathological conditions (see, e.g. Woodcock *et al.* 1998; Mackenzie *et al.* 2002), the spatio-temporal organization of IP_3-dependent Ca^{2+} release and the specific mechanisms by which IP_3 signalling modulates Ca^{2+} handling in atrial myocytes is not clear.

Methods

Cell isolation

The procedure for cell isolation was approved by the Institutional Animal Care and Use Committee of Loyola University Chicago, Stritch School of Medicine. Adult mongrel cats of either sex (19 animals were used in this study) were anaesthetized with thiopental sodium (30 mg kg^{-1} I.P.). Following thoracotomy hearts were quickly excised, mounted on a Langendorff apparatus, and retrogradely perfused with collagenase-containing solution at 37°C according to the method previously described (Kockskämper & Blatter, 2002; Sheehan & Blatter, 2003). All experiments were carried out at room temperature (22–24°C).

$[Ca^{2+}]_i$ measurements

$[Ca^{2+}]_i$ was measured in intact and permeabilized atrial myocytes with fluorescence laser scanning confocal microscopy. Intact atrial myocytes were loaded with the Ca^{2+} indicator fluo-4 by 20 min incubation in Tyrode solution containing 20 μM fluo-4 acetoxymethyl ester (fluo-4/AM; Molecular Probes, Eugene, OR, USA) at room temperature. Cells were superfused continuously (1 ml min^{-1}) with normal Tyrode solution (composition in mM: NaCl 140; KCl 4; $CaCl_2$ 2; $MgCl_2$ 1; glucose 10; Hepes 10; pH 7.4 adjusted with NaOH). Fifteen to twenty minutes was allowed for de-esterification of the dye. $[Ca^{2+}]_i$ measurements were performed with a laser scanning confocal microscope (Radiance 2000 MP, Bio-Rad, UK) equipped with a × 40 oil-immersion objective lens (N.A. = 1.3). Fluo-4 (and fluo-3 in permeabilized cells; see below) was excited with the 488 nm line of an argon ion laser and fluorescence was measured at wavelengths >515 nm. Images were acquired in the linescan mode (3 or 6 ms per scan; pixel size 0.3 μm). Whole-cell $[Ca^{2+}]_i$ transients were obtained by averaging the entire cellular fluorescence signal from the line scanned. $[Ca^{2+}]_i$ transients are presented as background-subtracted normalized fluorescence (F/F_0) where F is the fluorescence intensity and F_0 is resting fluorescence recorded under steady-state conditions at the beginning of an experiment. $[Ca^{2+}]_i$ transients were evoked by electrical field stimulation (0.5 Hz). Ca^{2+} sparks were detected and quantified in terms of amplitude, spatial width and frequency using an automated detection algorithm (Cheng *et al.* 1999). Ca^{2+} spark frequencies are expressed as number of observed sparks per second and per 100 μm of scanned distance in the confocal linescan mode (sparks s^{-1} (100 μm)$^{-1}$). Atrial myocytes were permeabilized with saponin (Zima *et al.* 2003). First, the cells were suspended in a solution containing (mM): potassium aspartate 100; KCl 20; EGTA 0.5; $MgCl_2$ 0.75; Hepes 10; pH 7.2 (KOH) and placed in the experimental chamber (final volume 50 μl) for 15 min. The cell surface membrane was permeabilized by adding 0.005% (w/v) saponin for 30 s. After 30 s the bath solution was exchanged for a saponin-free internal solution composed of (mM): potassium aspartate 100; KCl 15; KH_2PO_4 5; MgATP 5; EGTA 0.4; $CaCl_2$ 0.12; $MgCl_2$ 0.75; phosphocreatine 10; creatine phosphokinase 5 U ml^{-1}; dextran (M_r: 40 000) 8%; Hepes 10; fluo-3 potassium salt 0.04; pH 7.2 (KOH). Free $[Ca^{2+}]$ and $[Mg^{2+}]$ of this solution were 100 nM and 1 mM, respectively (calculated using WinMAXC 2.05, Stanford University, CA, USA).

Drugs

IP_3 and adenophostin were obtained from Calbiochem, and 2-aminoethoxydiphenyl borate (2-APB), ET-1, heparin (M_r 6000) and tetracaine were from Sigma.

Data analysis

Data are presented as the mean ± S.E.M. of n measurements. Statistical comparisons between groups were performed with Student's t test.

Results

Endothelin effects on Ca^{2+} signals in intact atrial myocytes: involvement of IP_3 signalling

Neurohumoral stimuli (α-adrenergic agents, angiotensin II or endothelin) can cause an increase of $[IP_3]$ in atrial cells (Vogelsang *et al.* 1994). We used endothelin (ET-1), which binds to ET receptors (ET_A receptor subtype), to study the effect of IP_3-dependent Ca^{2+} signalling during E-C coupling in intact adult mammalian atrial myocytes. In electrically stimulated cells ET-1 (100 nM; 10 min exposure time) caused an increase in diastolic $[Ca^{2+}]_i$ by 61 ± 11% ($P < 0.05$; observed in 93% of the cells tested; $n =$ 14 cells). The amplitude (Fig. 1*A*) of electrically evoked

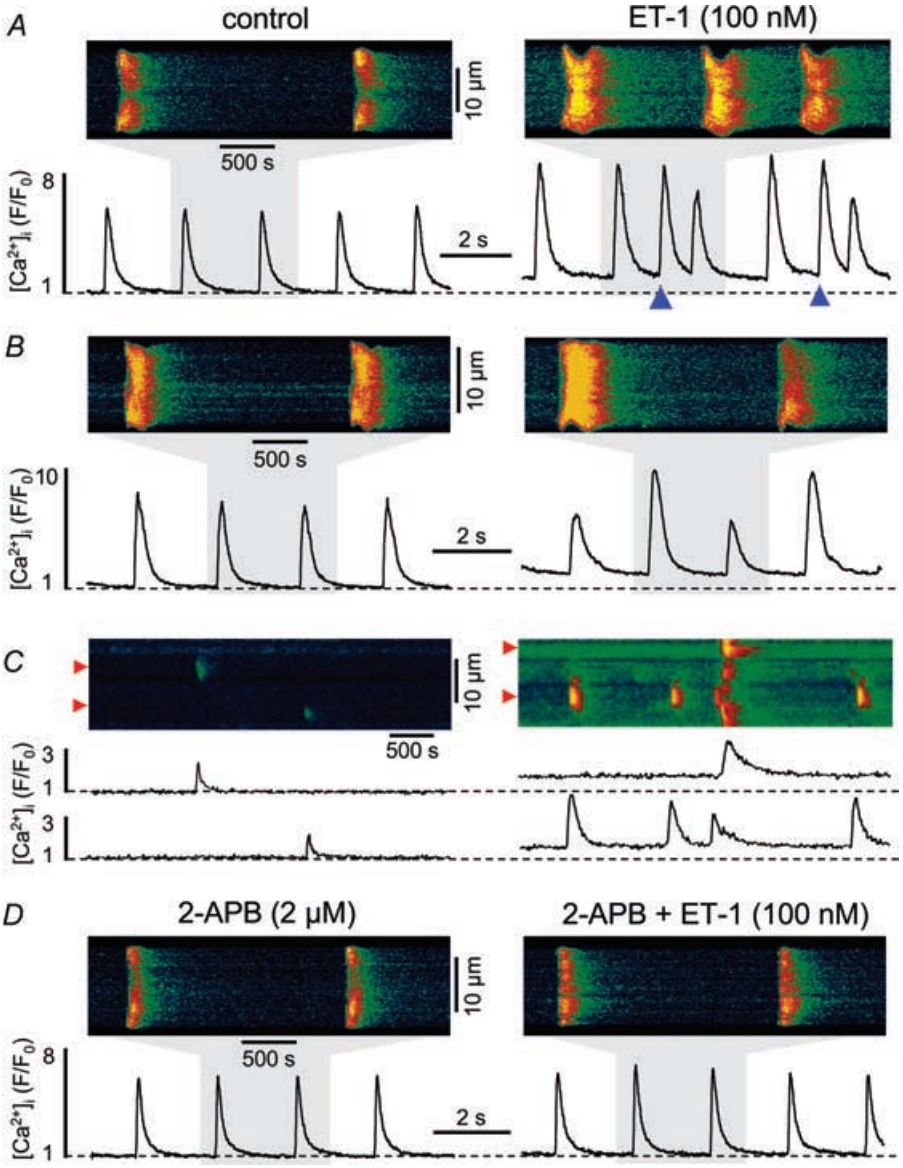

Figure 1. Effects of endothelin-1 (ET-1) on Ca^{2+} signalling in intact cat atrial myocytes
Confocal linescan images and spatially averaged $[Ca^{2+}]_i$ transients recorded from field-stimulated (0.5 Hz) atrial myocytes. *A*, ET-1 (100 nM) increased diastolic $[Ca^{2+}]_i$ and amplitude of electrically evoked $[Ca^{2+}]_i$ transients. Spontaneous $[Ca^{2+}]_i$ transients and Ca^{2+} waves (marked by the blue triangles in the right panel) occurred between triggered transients in the presence of ET-1. The traces represent $[Ca^{2+}]_i$ expressed as normalized changes of fluo-4 fluorescence (F/F_0). *B*, ET-1 elicited Ca^{2+} alternans. *C*, confocal linescan images of spontaneous Ca^{2+} sparks (top) and selected subcellular $[Ca^{2+}]_i$ traces (F/F_0, averaged over a distance of 1 μm marked by the red triangles to the left of the images) under control conditions (left) and after application of ET-1 (right). ET-1 caused a significant increase in Ca^{2+} spark frequency and resting $[Ca^{2+}]_i$. *D*, the IP_3R inhibitor 2-APB (2 μM) prevented the effects of ET-1 on $[Ca^{2+}]_i$.

action potential-dependent $[Ca^{2+}]_i$ transients increased by 27 ± 8% ($P < 0.05$; 71% of the cells). This positive inotropic effect was typically seen after about 4 min of exposure to ET-1, and the maximum effect of ET-1 on Ca^{2+} signalling was observed after 6–8 min. Furthermore, ET-1 caused spontaneous $[Ca^{2+}]_i$ transients and Ca^{2+} waves (Fig. 1*A* and *C*; observed in 43% of the cells tested). A majority of cells developed Ca^{2+} alternans (Figs 1*B*; 64% of the cells). Ca^{2+} alternans occurred with a delay of 1–2 min after the first signs of an ET-1-induced positive inotropic effect and was stable until the end of exposure to ET-1. In unstimulated cells ET-1 increased the frequency of spontaneous RyR-dependent Ca^{2+} sparks (Fig. 1*C*) from 0.96 ± 0.16 to 3.5 ± 1.1 sparks s^{-1} $(100\,\mu m)^{-1}$ ($P < 0.05$; $n = 6$ cells). This effect of ET-1 was seen within the first minute of application of the agonist and was fully established after 6 min of exposure to ET-1. The membrane permeant IP_3R antagonist 2-APB (2–5 μM) prevented or abolished all ET-1 effects on $[Ca^{2+}]_i$ in atrial cells (Fig. 1*D*), suggesting that ET-1 effects were mediated by IP_3, presumably through IP_3-dependent Ca^{2+} release.

IP_3-dependent Ca^{2+} signals in permeabilized cardiac myocytes

We tested the effect of the physiological agonist IP_3 directly in saponin-permeabilized myocytes (Fig. 2*A*). IP_3 (20 μM) increased (Fig. 2*C*) basal $[Ca^{2+}]_i$ by 34 ± 4% ($P < 0.001$; $n = 12$) and Ca^{2+} spark frequency from 6.4 ± 0.7 to 9.7 ± 1.1 sparks s^{-1} $(100\,\mu m)^{-1}$ ($P < 0.01$; $n = 12$). However, IP_3 did not alter Ca^{2+} spark amplitude or duration. The latter suggests that IP_3 enhanced the probability of an SR Ca^{2+} release unit (cluster of RyRs) to liberate Ca^{2+} but did not change properties of the RyR cluster. Similar to IP_3, adenophostin (5 μM), a more potent IP_3 agonist with two orders of magnitude higher affinity not subject to cellular enzymatic degradation, also increased (Fig. 2*B* and *C*) basal $[Ca^{2+}]_i$ by 33 ± 7% ($P < 0.01$; $n = 6$) and raised the Ca^{2+} spark frequency from 5.4 ± 0.5 to 8.9 ± 0.6 sparks s^{-1} $(100\,\mu m)^{-1}$ ($P < 0.01$; $n = 6$). The effects on basal $[Ca^{2+}]_i$ and Ca^{2+} sparks were seen rapidly (<1 min) after exposure to the agonists, but required approximately 5 min to develop fully. In contrast to atrial myocytes IP_3 failed to change the frequency and properties of Ca^{2+} sparks in cat ventricular cells ($n = 6$ cells) indicating that the IP_3 effect on Ca^{2+} signalling was specific to atrial myocytes (Fig. 2*D*).

To assure that the observed effects of IP_3 were indeed due to IP_3-dependent Ca^{2+} release from the SR we applied the known IP_3R antagonists heparin as well as 2-APB. In the presence of heparin (0.5 mg ml^{-1}) IP_3 (50 μM) failed to increase basal $[Ca^{2+}]_i$ and Ca^{2+} spark frequency (Fig. 3*A*). Similarly, the action of IP_3 on basal $[Ca^{2+}]_i$ and Ca^{2+} sparks was also prevented by 2-APB (5 μM; Fig. 3*B*). In addition, inhibition of IP_3Rs with 2-APB reversed the effects of IP_3 on basal $[Ca^{2+}]_i$ and Ca^{2+} spark frequency (Fig. 3*C*).

Elementary IP_3R-dependent Ca^{2+} release events in cardiac myocytes

Elementary non-propagating IP_3R-dependent Ca^{2+} release events, termed Ca^{2+} blips and puffs, have been observed in non-excitable cells such as oocytes (Parker & Yao, 1996), HeLa (Bootman *et al.* 1997) and vascular endothelial cells (Hüser & Blatter, 1997). They differ from RyR-mediated Ca^{2+} sparks in amplitude and kinetics, and have not been observed in cardiac myocytes, presumably because they are difficult to discern in the 'Ca^{2+} noise' from RyR-dominated Ca^{2+} release. We tested whether IP_3-dependent puff-like events occurred in conditions where Ca^{2+} release via RyRs was blocked. For this purpose permeabilized atrial myocytes revealing spontaneous Ca^{2+} spark activity were treated with the RyR inhibitor tetracaine (Györke *et al.* 1997). Tetracaine instead of ryanodine was used to block the RyR, because ryanodine locks RyRs into a subconductance state which can lead to depletion of the SR. In control experiments we confirmed the inhibition of RyR activity by tetracaine. Tetracaine (1 mM) reduced the open probability of the RyR channel on average by 98% ($P < 0.01$; $n = 3$) as measured with single channel recordings from RyRs incorporated into lipid bilayer (data not shown). Tetracaine also blocked spontaneous RyR-mediated Ca^{2+} sparks. Ca^{2+} spark frequency decreased from 6.0 ± 0.5 to 0.2 ± 0.1 sparks s^{-1} $(100\,\mu m)^{-1}$ ($P < 10^{-7}$; $n = 12$). After eliminating spontaneous Ca^{2+} sparks with tetracaine, permeabilized atrial myocytes were exposed to IP_3 (20 μM). Despite inhibition of RyRs, IP_3 caused a significant increase of basal $[Ca^{2+}]_i$ by 37 ± 7% ($P < 0.001$; $n = 6$). In addition, localized non-propagating $[Ca^{2+}]$ elevations appeared. Heparin completely abolished these Ca^{2+} release events. Adenophostin in the presence of tetracaine elicited the same type of elementary Ca^{2+} release events (Fig. 4*A*, bottom). Figure 4*B* shows averaged linescan images and $[Ca^{2+}]_i$ profiles of RyR-mediated Ca^{2+} sparks (control) and IP_3R-mediated elementary release events elicited with IP_3 and adenophostin, respectively. In summary (Fig. 4*C*, bottom) the IP_3R-dependent events had amplitudes which were 75–80% smaller than the average Ca^{2+} spark amplitude (see also surface plots of averaged RyR- and IP_3R-mediated elementary release events, top panel

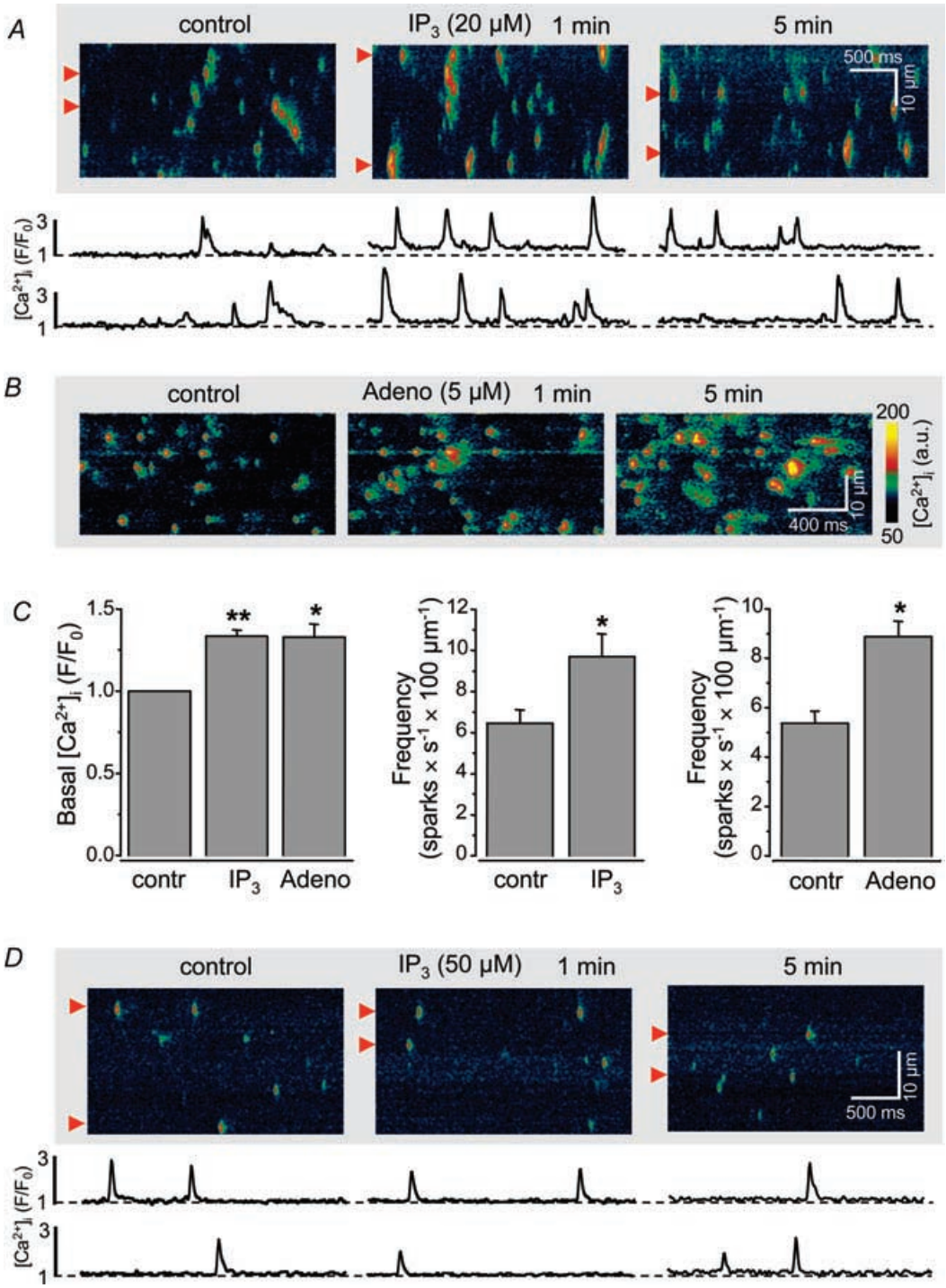

Figure 2. Effects of IP_3 and adenophostin on $[Ca^{2+}]_i$ in saponin-permeabilized atrial and ventricular myocytes

A, top, confocal linescan images (fluo-4 fluorescence images; a.u., arbitrary fluorescence intensity units) under control conditions and 1 and 5 min after exposure to 20 μM IP_3. Bottom, local subcellular changes of $[Ca^{2+}]_i$ (F/F_0 averaged over 1 μm indicated by the red triangles to the left of the images). *B*, effect of adenophostin (5 μM; same experimental conditions as in *A*. *C*, average data of the effects of IP_3 and adenophostin on basal $[Ca^{2+}]_i$ and Ca^{2+} spark frequency. Statistically different at $P < 0.01$ (*) and $P < 0.001$ (**). *A–C* reflect data obtained from atrial myocytes. *D*, IP_3 had no effect on basal $[Ca^{2+}]_i$ and frequency and properties of Ca^{2+} sparks in permeabilized cat ventricular myocytes, suggesting that the IP_3 effects were specific to atrial myocytes. $[Ca^{2+}]_i$ was measured with fluo-3 pentapotassium salt (fluo-3 bath concentration was 40 μM).

of Fig. 4*C*). On average IP_3R-mediated events were three to four times longer than Ca^{2+} sparks and the rise time was prolonged by approximately a factor of 2. The spatial spread of the two types of release events did not differ significantly. The differences in kinetics become evident when the average amplitudes were normalized (Fig. 4*B*, right). The first derivative of the $[Ca^{2+}]_i$ transient ($d(F/F_0)/dt$), which approximates the underlying Ca^{2+} flux (Sheehan & Blatter, 2003), revealed that the Ca^{2+} release flux of IP_3-dependent events was clearly smaller. On rare occasions small non-propagating Ca^{2+} release events were observed in the presence of tetracaine alone. These events were approximately three times smaller in amplitude than Ca^{2+} sparks recorded under control conditions, however, they revealed otherwise the same spatial and temporal characteristics (average Ca^{2+} spark properties in tetracaine: amplitude $\Delta F/F_0 = 0.67$; duration 26.6 ms; width 2.0 μm; rise time 17.2 ms) as regular Ca^{2+} sparks (compare to tabulated values in Fig. 4*C*). Thus, these rare events were different from those observed after addition of IP_3 and resulted from the opening of a smaller number of RyRs in a cluster of release channels. In summary, the IP_3-dependent elementary Ca^{2+} release events we observed in permeabilized atrial myocytes were distinctly different from RyR Ca^{2+} sparks and were reminiscent of Ca^{2+} puffs typically observed in non-excitable tissue where IP_3-dependent Ca^{2+} signalling is predominant (Parker & Yao, 1996; Berridge, 1997; Bootman *et al.* 1997; Hüser & Blatter, 1997).

Discussion

Atrial myocytes reveal two classes of elementary Ca^{2+} release events

In this study we show that elementary Ca^{2+} release events from RyRs and IP_3Rs coexist in atrial myocytes. Although available quantitative data on the spatio-temporal properties of Ca^{2+} sparks and Ca^{2+} puffs or blips vary considerably (see, e.g. summary in Bootman, 1996), distinct differences in amplitude and kinetics are described. IP_3R-dependent elementary release events have slower rise and decline kinetics, last longer and have a

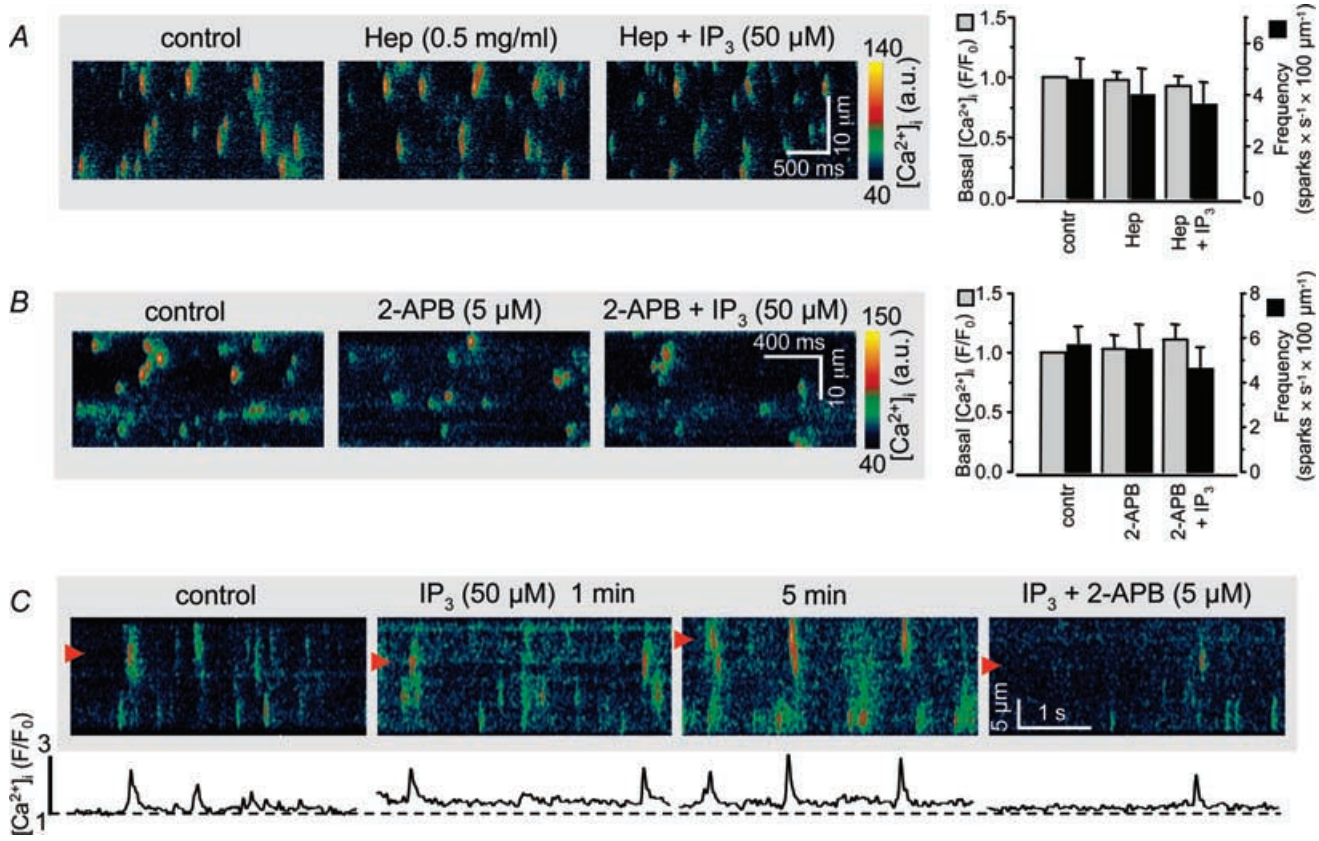

Figure 3. Effect of inhibitors of IP_3 receptors
A, preincubation of permeabilized atrial myocytes with heparin prevented the effect of IP_3 (50 μM) on basal $[Ca^{2+}]_i$ and Ca^{2+} sparks. *B*, same experiment as in *A* but with the IP_3R blocker 2-APB (5 μM). *C*, 2-APB reversed the increase of basal $[Ca^{2+}]_i$ and Ca^{2+} spark frequency induced by preceding exposure to IP_3.

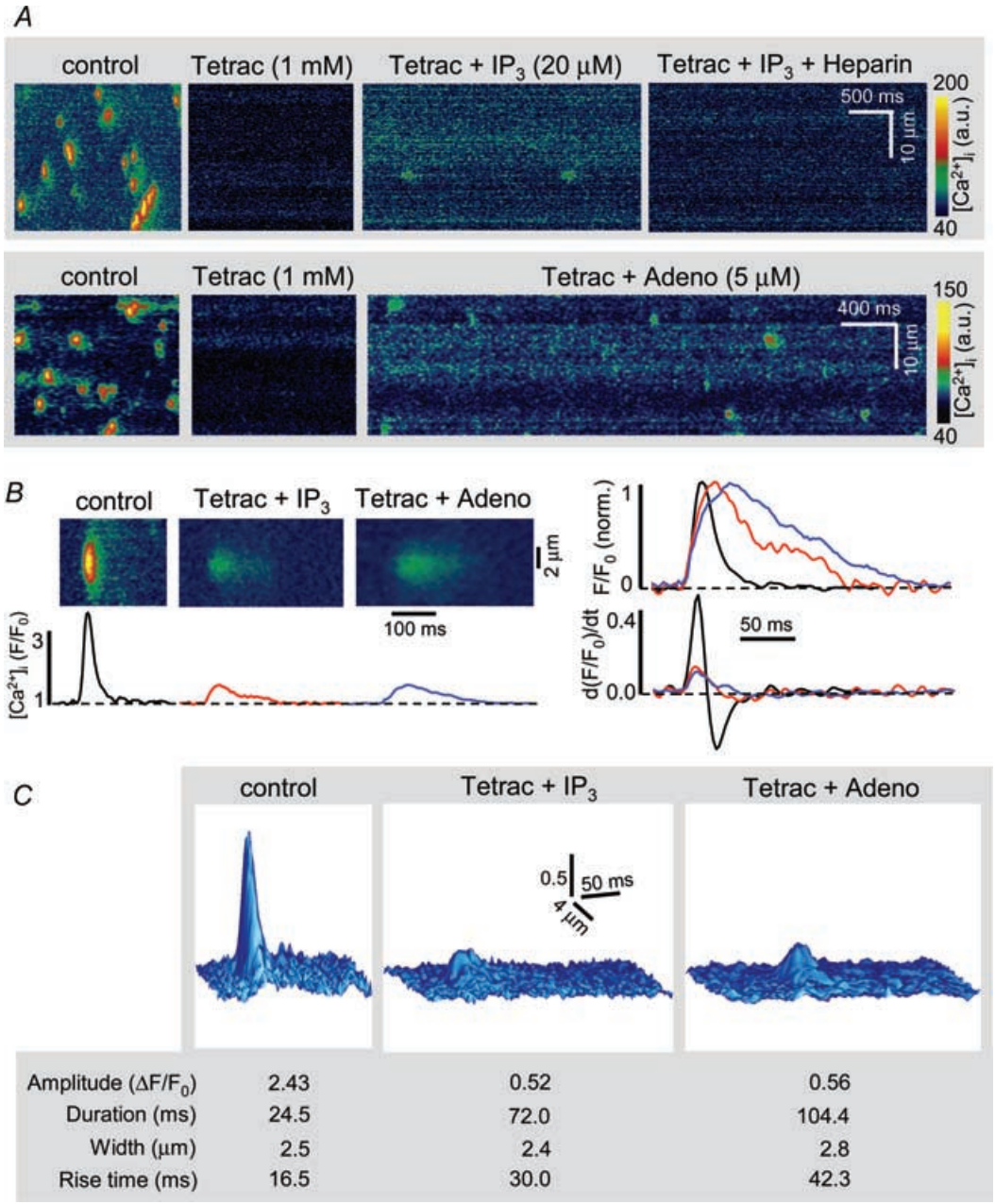

	control	Tetrac + IP_3	Tetrac + Adeno
Amplitude ($\Delta F/F_0$)	2.43	0.52	0.56
Duration (ms)	24.5	72.0	104.4
Width (µm)	2.5	2.4	2.8
Rise time (ms)	16.5	30.0	42.3

Figure 4. Elementary Ca^{2+} release events from IP_3Rs in atrial myocytes
A, confocal linescan images from permeabilized cat atrial myocytes. Top, tetracaine (1 mM) abolished spontaneous Ca^{2+} spark activity. In the presence of tetracaine, IP_3 (20 μM) caused an increase in basal $[Ca^{2+}]_i$ and the occurrence of non-propagating Ca^{2+} release events with significantly different amplitude and kinetics compared to Ca^{2+} sparks. Heparin abolished the elevation of basal $[Ca^{2+}]$ and Ca^{2+} release events. Bottom, localized Ca^{2+} release events elicited with adenophostin in the presence of tetracaine. *B*, left, average linescan images and F/F_0 traces of Ca^{2+} sparks (black), and IP_3- (red) and adenophostin- (blue) mediated Ca^{2+} release events. Right, normalized amplitudes of local $[Ca^{2+}]_i$ transients (F/F_0, norm.) and first derivatives ($d(F/F_0)/dt$). $d(F/F_0)/dt$ serves as a measure of the underlying Ca^{2+} release flux. *C*, surface plot representation of averaged linescan images of Ca^{2+} sparks and IP_3R-mediated Ca^{2+} release events from *B*. Bottom, table showing average values of Ca^{2+} release event amplitude ($\Delta F/F_0$), duration (measured at half maximum amplitude), spatial width (full width at half maximum amplitude) and rise time. 'Control' indicates RyR-mediated Ca^{2+} sparks recorded in the absence of tetracaine and IP_3R agonists.

smaller amplitude. The same observation was made in this study where the two types of release events could be compared directly. The IP_3-dependent release events differed from RyR-dependent Ca^{2+} sparks in all of these parameters in the same manner. The duration of the IP_3-dependent events observed in atrial myocytes compares fairly well with Ca^{2+} puffs observed in HeLa (Bootman *et al.* 1997) and vascular endothelial cells (Hüser & Blatter, 1997) which is in the range of 100–200 ms, compared to the duration of a Ca^{2+} spark (<50 ms; see, e.g. Bers 2001). Thus, the elementary IP_3R-dependent events recorded from atrial myocytes are clearly reminiscent of Ca^{2+} puffs observed in non-excitable tissues.

Cross-talk between IP_3R- and RyR-dependent Ca^{2+} release: modulation of CICR by IP_3

In atrial myocytes Ca^{2+} release from the SR during E-C coupling occurs primarily through RyRs. We have shown that in cat atrial myocytes inhibition of RyRs reduces the $[Ca^{2+}]_i$-transient amplitude by ~90% (Kockskämper *et al.* 2001; Sheehan & Blatter, 2003). Nonetheless, in atrial tissue IP_3-dependent Ca^{2+} release exerts an important modulatory role for Ca^{2+} signalling during E-C coupling by facilitating Ca^{2+} release via RyRs. IP_3-dependent Ca^{2+} release makes also a small direct contribution to the $[Ca^{2+}]_i$ transient although in quantitative terms this effect is likely to be small based on the small number of IP_3Rs and the magnitude of IP_3-dependent Ca^{2+} release events. Ca^{2+} affects the behaviour of both types of channels. Ca^{2+} is the primary activator of RyRs, and cytoplasmic as well as lumenal Ca^{2+} change the sensitivity of the release channel to CICR. The open probability (P_o) of the IP_3R type-2 (cardiac) shows a steep Ca^{2+} dependence in the range of 10–100 nM, but is rather Ca^{2+}-independent at $[Ca^{2+}] > 100$ nM (Ramos-Franco *et al.* 1998), i.e. at $[Ca^{2+}]$ encountered in cardiac cells at rest as well as during activation. Type-2 IP_3R has the highest sensitivity to IP_3, suggesting, together with its Ca^{2+}-independence at $[Ca^{2+}] > 100$ nM, that the cardiac IP_3R functions as a pure IP_3 sensor. This suggests that IP_3Rs are rather unaffected by Ca^{2+} release from RyR. In contrast, release of Ca^{2+} from IP_3Rs can impose critical changes of $[Ca^{2+}]_i$ in the microenvironment of the RyRs which facilitates CICR from neighbouring RyR Ca^{2+} release sites. In the present study we found IP_3-dependent release events in both, in subsarcolemmal as well as in deeper regions of the cell, suggesting that IP_3-dependent Ca^{2+} release may affect CICR from both junctional and non-junctional SR of atrial myocytes (Blatter *et al.* 2003; Sheehan & Blatter, 2003). In summary, IP_3 can exert a positive inotropic effect by enhancing Ca^{2+} release from the SR and contraction in a beat-to-beat fashion. This may indeed represent one of the mechanisms through which neurohumoral agents such as α-adrenergic agonists, angiotensin II or endothelin modulate cardiac Ca^{2+} signalling and contractility.

IP_3-dependent Ca^{2+} signalling and atrial arrhythmias

IP_3-dependent Ca^{2+} signalling has been implied in cardiac arrhythmias due to ischaemia and reperfusion injury, inflammatory processes and developing cardiac failure (see, e.g. Woodcock *et al.* 1998; Mackenzie *et al.* 2002). Our data lend direct support to the notion that IP_3-dependent Ca^{2+} release plays a causal role in the genesis of atrial arrhythmias. IP_3 caused spontaneous $[Ca^{2+}]_i$ transients and Ca^{2+} waves as well as Ca^{2+} alternans (Fig. 1), all disturbances in Ca^{2+} signalling related to cardiac arrhythmias (see Kockskämper & Blatter, 2002). Our observation that IP_3-dependent Ca^{2+} signalling is pivotal for atrial E-C coupling and is responsible for the pro-arrhythmogenic disturbances of cellular Ca^{2+} homeostasis suggests that therapeutic agents which target the IP_3R and the IP_3/Ca^{2+} signalling cascade may prove beneficial for the prevention and treatment of cardiac arrhythmias (Woodcock *et al.* 1998).

References

Berridge MJ (1997). Elementary and global aspects of calcium signalling. *J Physiol* **499**, 291–306.

Bers DM (2001). *Excitation-Contraction Coupling and Cardiac Contractile Force*, 2nd edn. Kluwer, Dordrecht, Netherlands.

Blatter LA, Hüser J & Rios E (1997). Sarcoplasmic reticulum Ca^{2+} release flux underlying Ca^{2+} sparks in cardiac muscle. *Proc Natl Acad Sci U S A* **94**, 4176–4181.

Blatter LA, Kockskämper J, Sheehan KA, Zima AV, Hüser J & Lipsius SL (2003). Local calcium gradients during excitation–contraction coupling and alternans in atrial myocytes. *J Physiol* **546**, 19–31.

Bootman MD (1996). Hormone-evoked subcellular Ca^{2+} signals in HeLa cells. *Cell Calcium* **20**, 97–104.

Bootman M, Niggli E, Berridge M & Lipp P (1997). Imaging the hierarchical Ca^{2+} signalling system in HeLa cells. *J Physiol* **499**, 307–314.

Cheng H, Song LS, Shirokova N, Gonzalez A, Lakatta EG, Rios E *et al.* (1999). Amplitude distribution of calcium sparks in confocal images: theory and studies with an automatic detection method. *Biophys J* **76**, 606–617.

Fabiato A (1986). Inositol (1,4,5)-trisphosphate induced release of Ca^{2+} from the sarcoplasmic reticulum of skinned cardiac cell. *Biophys J* **49**, 190a.

Györke S, Lukyanenko V & Györke I (1997). Dual effects of tetracaine on spontaneous calcium release in rat ventricular myocytes. *J Physiol* **500**, 297–309.

Harrison SN, Autelitano DJ, Wang BH, Milano C, Du XJ & Woodcock EA (1998). Reduced reperfusion-induced Ins(1,4,5)P_3 generation and arrhythmias in hearts expressing constitutively active α_{1B}-adrenergic receptors. *Circ Res* **83**, 1232–1240.

Hirata M, Suematsu E, Hashimoto T, Hamachi T & Koga T (1984). Release of Ca^{2+} from a non-mitochondrial store site in peritoneal macrophages treated with saponin by inositol 1,4,5-trisphosphate. *Biochem J* **223**, 229–236.

Hüser J & Blatter LA (1997). Elementary events of agonist-induced Ca^{2+} release in vascular endothelial cells. *Am J Physiol* **273**, C1775–C1782.

Jacobsen AN, Du XJ, Lambert KA, Dart AM & Woodcock EA (1996). Arrhythmogenic action of thrombin during myocardial reperfusion via release of inositol 1,4,5-triphosphate. *Circulation* **93**, 23–26.

Jaconi M, Bony C, Richards SM, Terzic A, Arnaudeau S, Vassort G *et al.* (2000). Inositol 1,4,5-trisphosphate directs Ca^{2+} flow between mitochondria and the endoplasmic/sarcoplasmic reticulum: a role in regulating cardiac autonomic Ca^{2+} spiking. *Mol Biol Cell* **11**, 1845–1858.

Kockskämper J & Blatter LA (2002). Subcellular Ca^{2+} alternans represents a novel mechanism for the generation of arrhythmogenic Ca^{2+} waves in cat atrial myocytes. *J Physiol* **545**, 65–79.

Kockskämper J, Sheehan KA, Bare DJ, Lipsius SL, Mignery GA & Blatter LA (2001). Activation and propagation of Ca^{2+} release during excitation–contraction coupling in atrial myocytes. *Biophys J* **81**, 2590–2605.

Lipp P, Laine M, Tovey SC, Burrell KM, Berridge MJ, Li W *et al.* (2000). Functional $InsP_3$ receptors that may modulate excitation-contraction coupling in the heart. *Curr Biol* **10**, 939–342.

Mackenzie L, Bootman MD, Laine M, Berridge MJ, Thuring J, Holmes A *et al.* (2002). The role of inositol 1,4,5-trisphosphate receptors in Ca^{2+} signalling and the generation of arrhythmias in rat atrial myocytes. *J Physiol* **541**, 395–409.

Marks AR (2000). Cardiac intracellular calcium release channels: role in heart failure. *Circ Res* **87**, 8–11.

Mouton R, Genade S, Huisamen B, Malan M & Lochner A (1992). The effect of ischaemia-reperfusion on [^{3}H]inositol phosphates and ins (1,4,5) P_3 levels in cardiac atria and ventricles – a comparative study. *Mol Cell Biochem* **115**, 195–202.

Nosek TM, Williams MF, Zeigler ST & Godt RE (1986). Inositol trisphosphate enhances calcium release in skinned cardiac and skeletal muscle. *Am J Physiol* **250**, C807–C811.

Parker I & Yao Y (1996). Ca^{2+} transients associated with openings of inositol trisphosphate-gated channels in *Xenopus* oocytes. *J Physiol* **491**, 663–668.

Perez PJ, Ramos-Franco J, Fill M & Mignery GA (1997). Identification and functional reconstitution of the Type-2 $InsP_3$ receptor from ventricular cardiac myocytes. *J Biol Chem* **272**, 23961–23969.

Poindexter BJ, Smith JR, Buja LM & Bick RJ (2001). Calcium signaling mechanisms in dedifferentiated cardiac myocytes: comparison with neonatal and adult cardiomyocytes. *Cell Calcium* **30**, 373–382.

Ramos-Franco J, Fill M & Mignery GA (1998). Isoform-specific function of single inositol 1,4,5-trisphosphate receptor channels. *Biophys J* **75**, 834–839.

Rosemblit N, Moschella MC, Ondriasa E, Gutstein DE, Ondrias K & Marks AR (1999). Intracellular calcium release channel expression during embryogenesis. *Dev Biol* **206**, 163–177.

Sheehan KA & Blatter LA (2003). Regulation of junctional and non-junctional sarcoplasmic reticulum calcium release in excitation–contraction coupling in cat atrial myocytes. *J Physiol* **546**, 119–135.

Vogelsang M, Broede-Sitz A, Schafer E, Zerkowski HR & Brodde OE (1994). Endothelin ET_A-receptors couple to inositol phosphate formation and inhibition of adenylate cyclase in human right atrium. *J Cardiovasc Pharmacol* **23**, 344–347.

Woodcock EA, Lambert KA, Phan T & Jacobsen AN (1997). Inositol phosphate metabolism during myocardial ischemia. *J Mol Cell Cardiol* **29**, 449–460.

Woodcock EA, Matkovich SJ & Binah O (1998). Ins(1,4,5)P_3 and cardiac dysfunction. *Cardiovasc Res* **40**, 251–256.

Yamada J, Ohkusa T, Nao T, Ueyama T, Yano M, Kobayashi S *et al.* (2001). Up-regulation of inositol 1,4,5 trisphosphate receptor expression in atrial tissue in patients with chronic atrial fibrillation. *J Am Coll Cardiol* **37**, 1111–1119.

Zima AV, Kockskämper J, Mejia-Alvarez R & Blatter LA (2003). Pyruvate modulates cardiac sarcoplasmic reticulum Ca^{2+} release in rats via mitochondria-dependent and -independent mechanisms. *J Physiol* **550**, 765–783.

Acknowledgements

Supported by NIH grant HL-62231 (LAB). We wish to thank Drs S. L. Lipsius and G. A. Mignery for helpful discussions. The technical assistance of A. Pezalla is gratefully acknowledged.